Journal of Sound and Vibration (1999) **225**(2), 211–238
Article No. jsvi.1999.2236, available online at http://www.idealibrary.com on IDEAL®

TRAILING EDGE NOISE AT LOW MACH NUMBERS

M. S. HOWE

College of Engineering, Boston University, 110 *Cummington Street, Boston, MA* 02215, *USA*

(*Received* 1 *September* 1998)

A review is made of the diffraction theory of the trailing edge noise generated by a flat-plate airfoil of zero-thickness and non-compact chord, according to which the sound is attributed to the scattering of a "frozen" pattern of turbulence wall pressure swept over the edge in the mean flow. Extension is made to determine the sound produced by very low Mach number flow over the edge of an airfoil of finite thickness. In applications it is desirable to represent the noise in terms of a surface integral over the airfoil involving a Green's function and a metric of the edge flow that can be calculated locally using the equations of motion of an *incompressible* fluid. It is argued that the appropriate metric for a rigid airfoil is the incompressible "upwash" velocity (determined by the Biot–Savart induction formula applied to the boundary layer vorticity outside the viscous sublayer), and *not* the surface pressure. Formulae for calculating the noise are given when the airfoil thickness is acoustically compact, and for both three- and two-dimensional edge flows.

The theory is illustrated by a detailed discussion of a two-dimensional vortex flow over an airfoil with a rounded trailing edge. The problem is simple enough to be treated analytically, yet is also suitable for validating computational edge noise schemes.

1. INTRODUCTION

The "self-noise" generated by an airfoil in a nominally steady, high Reynolds number flow is attributed to the instability of the airfoil boundary layers and their interactions with the trailing edge [1–3]. The edge is usually a source of high-frequency sound associated with smaller-scale components of the boundary layer turbulence. Low-frequency contributions from a trailing edge, that may in practice be related to large-scale vortical structures shed from an upstream appendage, are small because the upwash velocity they produce in the neighborhood of the edge tends to be cancelled by that produced by vorticity shed from the edge [4, 5]. If the surface S of the airfoil is *rigid*, and is at rest in a mean stream, the far-field acoustic pressure $p'(\mathbf{x}, t) \equiv p(\mathbf{x}, t) - p_0$ at position $\mathbf{x}$ and time t [$p(\mathbf{x}, t)$ being the pressure and p_0 its mean value in the acoustic far field] is given formally by Curle's [6, 7] formula

$$p'(\mathbf{x}, t) = \frac{\partial^2}{\partial x_i \partial x_j} \int_V [T_{ij}] \frac{\mathrm{d}^3\mathbf{y}}{4\pi |\mathbf{x} - \mathbf{y}|} - \frac{\partial}{\partial x_i} \oint_S [p'_{ij}] \frac{\mathrm{d}S_j(\mathbf{y})}{4\pi |\mathbf{x} - \mathbf{y}|}, \quad |\mathbf{x}| \to \infty, \qquad (1)$$

0022-460X/99/320211 + 28 $30.00/0

where the first integral is over the volume V occupied by the fluid, the surface element dS_j is directed into V,

$$p'_{ij} = (p - p_0)\delta_{ij} - \sigma_{ij}, \tag{2}$$

and σ_{ij} is the viscous stress tensor. The square brackets [ ] in equations (1) denote evaluation of the contents at the retarded time $t - |\mathbf{x} - \mathbf{y}|/c_0$, where c_0 is the speed of sound. The direct sound generated by the turbulence *quadrupoles* [8, 9] is represented by the first integral in equation (1). At low Mach numbers (e.g. underwater) $T_{ij} \approx \rho_0 v_i v_j$ (ρ_0 and $\mathbf{v}$ being respectively the mean fluid density and the velocity), and the quadrupole noise is usually negligible compared with that from the edge. The latter is contained in the surface integral in equation (1), and for an *acoustically compact* surface (for example, an airfoil whose chord is much smaller than the typical acoustic wavelength), the edge noise is equivalent to that generated by a distribution of *dipoles* on S, whose strength per unit area is the unsteady surface pressure [8, 9]. In that case the ratio of the acoustic powers generated by the edge and the volume quadrupoles $\sim O(1/M^2)$, where $M \sim v/c_0 \ll 1$ is the characteristic Mach number [6]. At high frequencies, when it is not permissible to assume the chord to be compact, the relative efficiency of the edge noise is increased to $O(1/M^3)$ [10].

For the compact chord airfoil the dipole strengths can be determined to a sufficient approximation for use in equation (1) by a preliminary calculation of the flow near the edge in which the influence of compressibility is ignored. However, although equation (1) is exact for a non-compact airfoil, it is not permissible to neglect compressibility when specifying the dipole strengths in the surface integral. Therefore, edge noise predictions have traditionally been made by one of two alternative procedures. In the first, it is assumed that the trailing edge is well approximated by a semi-infinite, rigid plate. A calculation is then performed in which the free-field *hydrodynamic* pressure p_I, say, generated by the boundary layer turbulence is *diffracted* by the edge. If p_I were known exactly this procedure would yield an accurate prediction of the edge generated sound. Hitherto, it has not been possible to prescribe with sufficient accuracy the influence of the edge on the hydrodynamic pressure, and it has usually been assumed that the turbulence is swept past the edge by the mean flow as a *frozen* distribution of vorticity [1, 11–15]. In the second method, the noise is calculated by the acoustic analogy theory of Lighthill [8, 9] using a *compact* Green's function tailored to the trailing edge geometry [16, 17] [as opposed to the free space Green's function used in Curle's equation (1)]. The sound can then be expressed directly in terms of the vorticity in the edge flow (calculated as if the flow is incompressible); this approach also enables the frozen approximation of the first method to be extended to more complicated trailing edge geometries [17].

Modern computational procedures will soon yield accurate predictions of the high Reynolds number hydrodynamic motion near a trailing edge, and it is appropriate to re-evaluate the kind of numerical data that will be required to make confident predictions of the farfield sound. We have suggested above that an incompressible approximation to the surface pressure is *not* sufficient when the

surface is not compact. This is because a non-compact body extends into the acoustic far field, and any representation of the sound as a Curle (or Kirchhoff) type of surface integral must ensure that the boundary conditions on the surface continue to be satisfied in the far field. This can be done either by using a Green's function tailored to the airfoil characteristics or [as in equation (1)] by using the free-space Green's function, but with p'_{ij} known to the required precision *in the acoustic domain*. In the latter case, the dipole strength must be prescribed with full account taken of compressibility, which is not normally possible because it presupposes a knowledge of the acoustic field at the surface [18]. In fact, the dipole strength can safely be estimated from an incompressible edge flow model only when the airfoil is acoustically compact. In general, the surface source strength turns out to depend on the *upwash* produced by the unsteady flow. When this is known (in an incompressible approximation), the edge noise can be found by using an acoustic Green's function whose normal derivative vanishes on the rigid surface of the airfoil.

In this paper, the thin-plate diffraction theory of trailing edge noise is first reviewed (section 2), and predictions are used to exhibit explicitly the failure of approximations based on equation (1). The general edge noise problem at low Mach numbers is then formulated in terms of the theory of vortex sound, and it is demonstrated how the sound can be determined from an incompressible approximation to the "upwash" velocity (section 3). The theory is illustrated by a detailed application (section 4) to determine the noise produced in a low Mach number vortex flow past the rounded trailing edge of a thick airfoil.

2. THIN-PLATE MODEL OF TRAILING EDGE NOISE

2.1. DIFFRACTION THEORY [11, 12]

Consider turbulent trailing edge flow over the *upper* surface $x_2 = +0$ of the rigid half-plane $x_1 < 0$, $x_2 = 0$, where the main stream outside the boundary layers has low subsonic speed U in the x_1-direction (Figure 1). The calculation of the edge noise is formulated as a scattering or diffraction problem, in which the pressure p_I, say, that would be produced by the same turbulent flow if the surface were absent, is scattered by the edge. The scattered pressure p' includes both acoustic and hydrodynamic components, the latter accounting for the modification of the nearfield pressure by the surface. The condition that the normal velocity vanishes on the half-plane is taken in the high Reynolds number approximation

$$\partial p_I/\partial x_2 + \partial p'/\partial x_2 = 0 \quad \text{on S}, \tag{3}$$

where S denotes the "upper" and "lower" surfaces ($x_1 < 0$, $x_2 = \pm 0$). In turbulence-free regions, and when the mean stream Mach number $M = U/c_0$ is very small, pressure fluctuations $p(\mathbf{x}, \omega)$ of frequency ω (with suppressed time factor

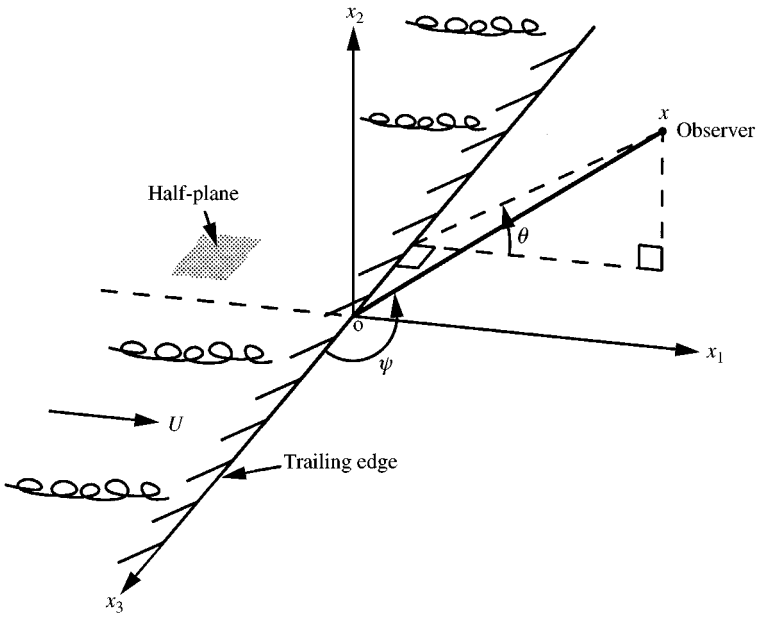

Figure 1. Co-ordinates for trailing edge noise.

$e^{-i\omega t}$) satisfy the Helmholtz equation

$$(\nabla^2 + \kappa_0^2)p = 0, \tag{4}$$

where $\kappa_0 = \omega/c_0$ is the acoustic wavenumber. The presence of the boundary layer and the turbulence are ignored except insofar as they are responsible for the pressure p_I; in particular $p'(\mathbf{x}, \omega)$ is assumed to satisfy equation (4) everywhere, and the scattering of sound by the shear flow is neglected. This approximation is not valid at very high frequencies when the acoustic wavelength is comparable to the thickness of the boundary layer.

The pressure $p_I(\mathbf{x}, \omega)$ must be an outgoing solution of Helmholtz's equation in $x_2 \leqslant 0$, in the region "below" the boundary layer sources; on $x_2 = 0$, p_I is equal to *half* the boundary layer *blocked pressure* p_s that the same turbulence would exert on an infinite plane wall at $x_2 = +0$, and we can write

$$p_I(\mathbf{x}, \omega) = \frac{1}{2}\int_{-\infty}^{\infty} p_s(\mathbf{k}, \omega)e^{i(\mathbf{k}, \mathbf{x} - \gamma(k_1)x_2)}\, dk_1\, dk_3, \quad x_2 \leqslant 0, \ \mathbf{k} = (k_1, 0, k_3), \tag{5}$$

where $\gamma(k) = \sqrt{\kappa_0^2 - k^2}$ is either real with sign sgn(ω) or positive imaginary. The problem of calculating p' now reduces to the determination of the scattered pressure [from equations (3) and (4)] produced by the interaction of each Fourier component $\frac{1}{2}p_s(\mathbf{k}, \omega)e^{i(\mathbf{k}, \mathbf{x} - \gamma(k)x_2)}$ of p_I with S.

The calculation can be performed by the Wiener–Hopf procedure [19], which supplies the following representation of the total perturbation pressure (which is

finite at the edge of the half-plane):

$$p(\mathbf{x},\omega)=\frac{1}{2}\int_{-\infty}^{\infty}p_s(\mathbf{k},\omega)\mathrm{e}^{\mathrm{i}(\mathbf{k},\mathbf{x}+\gamma(k)|x_2|)}\,\mathrm{d}k_1\,\mathrm{d}k_3$$

$$-\frac{\operatorname{sgn}(x_2)}{4\pi\mathrm{i}}\int_{-\infty}^{\infty}\frac{p_s(\mathbf{k},\omega)\sqrt{(\kappa_0^2-k_3^2)^{1/2}+k_1}}{\sqrt{(\kappa_0^2-k_3^2)^{1/2}+K_1}\,(K_1-k_1+\mathrm{i}0)}$$

$$\times\mathrm{e}^{\mathrm{i}(K_1x_1+k_3x_3+\gamma(K)|x_2|)}\,\mathrm{d}K_1\,\mathrm{d}k_1\,\mathrm{d}k_3, \tag{6}$$

where $K=\sqrt{K_1^2+k_3^2}$. The first integral represents the direct pressure p_I (generated by the boundary layer "in the absence of S"), and is strictly valid only outside the boundary layer in $x_2\leqslant 0$ or $x_2>\delta$, where δ is the boundary layer thickness.

The integration with respect to K_1 can be performed explicitly when $x_2\to\pm 0$. It is zero in the wake ($x_1\geqslant 0$), where the scattered pressure vanishes. For $x_1<0$ the integration contour is displaced to $-\mathrm{i}\infty$ in the K_1-plane, capturing the residue contribution from the pole at $K_1=k_1-\mathrm{i}0$ and an integral along the branch cut of $\sqrt{(\kappa_o^2-k_3^2)^{1/2}+K_1}$, which extends from $-(\kappa_0^2-k_3^2)^{1/2}$, just below the real axis, to $-\mathrm{i}\infty$. The branch-cut integral can be expressed in terms of the error function $\operatorname{erf}(x)=(2/\sqrt{\pi})\int_0^x\mathrm{e}^{-\lambda^2}\,\mathrm{d}\lambda$ [20]. The total surface pressure is then found to be

$$p(x_1,\pm 0,x_3,\omega)=\frac{1}{2}\iint_{-\infty}^{\infty}p_s(\mathbf{k},\omega)$$

$$\times[1\pm\operatorname{erf}(\mathrm{e}^{-\mathrm{i}\pi/4}|x_1|^{1/2}\sqrt{(\kappa_o^2-k_3^2)^{1/2}+k_1})]\,\mathrm{e}^{\mathrm{i}\mathbf{k},\mathbf{x}}\,\mathrm{d}^2\mathbf{k},\quad x_1<0. \tag{7}$$

The argument of the error function has positive real part for all real values of k_1, so that the error function ≈ 1 as $x_1\to-\infty$. Thus, $p\to 0$ on the lower surface ($x_2=-0$) far upstream of the edge, whereas $p\to p_s$ on the surface $x_2=+0$ exposed to the turbulent stream. This occurs at distances upstream of the edge exceeding the characteristic eddy dimension. If the impinging boundary layer turbulence is assumed to be frozen during convection over the edge, measurements of the blocked pressure p_s several boundary layer thicknesses upstream of the edge can be used in the second integral of equation (6) to predict the edge noise.

At large distances from the edge the integrations with respect to K_1 and k_3 in the second integral of equation (6) may be performed by the method of stationary phase [19, 21]. This yields the edge-scattered acoustic pressure in the Chase–Chandiramani [11, 12] form,

$$p'(\mathbf{x},\omega)\approx\frac{\kappa_0^{1/2}\sin^{1/2}\psi\sin(\theta/2)\mathrm{e}^{\mathrm{i}\kappa_0|\mathbf{x}|}}{\sqrt{2}|\mathbf{x}|}\int_{-\infty}^{\infty}$$

$$\times\frac{\sqrt{\kappa_0\sin\psi+k_1}}{(\kappa_0x_1/|\mathbf{x}|-k_1)}p_s(k_1,\kappa_o\cos\psi,\omega)\,\mathrm{d}k_1,\quad|\mathbf{x}|\to\infty, \tag{8}$$

where the angles θ,ψ defining the radiation direction $\mathbf{x}/|\mathbf{x}|$ are indicated in Figure 1.

The integrand in this formula is singular at $k_1 = \kappa_o x_1/|\mathbf{x}|$, where the stationary-phase approximation breaks down. However, this occurs when k_1 lies in the *acoustic domain*, i.e., for a blocked pressure Fourier component $p_s(k_1, \kappa_o \cos\psi, \omega)$ that actually represents a sound wave generated by the boundary layer quadrupoles in the absence of the edge. Such contributions can be neglected at small Mach numbers. When the blocked surface pressure is regarded as entirely *hydrodynamic*, the remaining integral in equation (8) is dominated by wavenumbers $k_1 \sim \omega/U \gg \kappa_o$, and equation (8) reduces to

$$p'(\mathbf{x},\omega) \approx \frac{-\kappa_o^{1/2}\sin^{1/2}\psi \sin(\theta/2)\,\mathrm{e}^{\mathrm{i}\kappa_o|\mathbf{x}|}}{\sqrt{2}|\mathbf{x}|}\int_{-\infty}^{\infty}\frac{p_s(k_1,0,\omega)\,\mathrm{d}k_1}{\sqrt{k_1+\mathrm{i}0}},\ |\mathbf{x}|\to\infty. \tag{9}$$

This representation is suitable for expressing of the edge noise in terms of the hydrodynamic (i.e., *incompressible*) component of the blocked pressure measured upstream of the edge.

This is usually done by referring $p_s(k_1,0,\omega)$ to the blocked surface pressure wavenumber-frequency spectrum $\mathrm{P}(\mathbf{k},\omega)$ [22]. It is assumed that a finite section $-\frac{1}{2}L < x_3 < \frac{1}{2}L$, say, of the trailing edge is wetted by the turbulent flow, where L is much larger than the boundary layer thickness δ. Then, for statistically stationary turbulence

$$\langle p_s(k_1,0,\omega)\,p_s^*(k_1',0,\omega')\rangle \approx (L/2\pi)\,\delta(\omega-\omega')\delta(k_1-k_1')\mathrm{P}(k_1,0,\omega),\quad L\gg\delta, \tag{10}$$

where the angle brackets $\langle\ \rangle$ represent an ensemble average, and the asterisk denotes complex conjugate. The acoustic pressure frequency spectrum $\Phi(\mathbf{x},\omega)$ of the edge noise [defined such that $\langle p'^2(\mathbf{x},\mathbf{t})\rangle = \int_0^\infty \Phi(\mathbf{x},\omega)\,\mathrm{d}\omega$] is then calculated from equation (9) to be given by

$$\Phi(\mathbf{x},\omega) \approx \frac{\omega L \sin^2(\theta/2)\sin\psi}{2\pi c_0|\mathbf{x}|^2}\int_{-\infty}^{\infty}\frac{\mathrm{P}(k_1,0,\omega)\,\mathrm{d}k_1}{|k_1|},\quad M\ll 1,\ |\mathbf{x}|\to\infty. \tag{11}$$

The peak acoustic pressures are radiated in the "forward" direction $\theta = \pm\pi$. Numerical predictions are made by introducing a convenient empirical model for $P(\mathbf{k},\omega)$ (see, e.g. references [22, 23]), although this will not be discussed here.

2.2. APPLICATION OF CURLE'S EQUATION

To derive these results from Curle's representation (1), the first, quadrupole, integral on the right is discarded, and p'_{ij} is approximated by $(p-p_0)\delta_{ij}$ at high Reynolds numbers. Then for each component of the sound of frequency ω,

$$p'(\mathbf{x},\omega) \approx -\frac{\partial}{\partial x_2}\int_{-\infty}^{\infty}\mathrm{d}y_3\int_{-\infty}^{0}[p(y_1,y_3)]\,\frac{\mathrm{e}^{\mathrm{i}\kappa_o|\mathbf{x}-\mathbf{y}|}}{4\pi|\mathbf{x}-\mathbf{y}|}\,\mathrm{d}y_1,\quad \mathbf{y}=(y_1,0,y_3), \tag{12}$$

where

$$[p(x_1, x_3)] = p(x_1, +0, x_3, \omega) - p(x_1, -0, x_3, \omega) \tag{13}$$

is the pressure jump across the half-plane.

At large distances from the wetted edge,

$$\frac{\partial}{\partial x_2}\left(\frac{e^{i\kappa_o|\mathbf{x}-\mathbf{y}|}}{4\pi|\mathbf{x}-\mathbf{y}|}\right) \approx \frac{i\kappa_o x_2 e^{i\kappa_o|\mathbf{x}|}}{4\pi|\mathbf{x}|^2} e^{-i\kappa_o \mathbf{x}\cdot\mathbf{y}/|\mathbf{x}|},$$

so that (because $[p(y_1, y_3)] \equiv 0$ for $y_1 > 0$)

$$p'(\mathbf{x}, \omega) \approx \frac{-i\kappa_o \sin\psi \sin\theta e^{i\kappa_o|\mathbf{x}|}}{4\pi|\mathbf{x}|} \int_{-\infty}^{\infty} dy_3 \int_{-\infty}^{\infty} [p(y_1, y_3)] e^{-i\kappa_o \mathbf{x}\cdot\mathbf{y}/|\mathbf{x}|} dy_1$$

$$= \frac{-\pi i\kappa_o \sin\psi \sin\theta}{|\mathbf{x}|} [\hat{p}(\kappa_o x_1/|\mathbf{x}|, \kappa_o x_3/|\mathbf{x}|)] e^{i\kappa_o|\mathbf{x}|}, \quad |\mathbf{x}| \to \infty, \tag{14}$$

where

$$[\hat{p}(k_1, k_3)] = \frac{1}{(2\pi)^2} \int_{-\infty}^{\infty} dy_3 \int_{-\infty}^{\infty} [p(y_1, y_3)] e^{-i(k_1 y_1 + k_3 y_3)} dy_1. \tag{15}$$

The first line of equation (14) implies that the principal contribution to the integral is from those components of $[p(y_1, y_3)]$ with length scales $\sim O(1/\kappa_o)$. In other words, a correct evaluation of the integral requires the retention of phase information in $[p]$ characterizing fluctuations in the surface pressure over distances of the order of the acoustic wavelength, which typically exceeds the scale of the hydrodynamic motions by a factor $1/M \gg 1$. In this integral phase interference with the exponential factor $e^{-i\kappa_o \mathbf{x}\cdot\mathbf{y}/|\mathbf{x}|}$ is responsible for correcting the directivity of the sound from that of a free-field dipole $\sim \sin\psi \sin\theta \equiv \cos\Theta$ (Θ being the angle between $\mathbf{x}/|\mathbf{x}|$ and the x_2-axis) orientated normal to the airfoil, to $\sin^{1/2}\psi \sin(\theta/2)$, which conforms to the rigid-body surface condition ($\partial p'/\partial x_n = 0$) in the far field.

If an attempt is made to approximate the surface pressure jump $[p(y_1, y_3)]$ in Curle's formula (12) by its value for incompressible flow, it would be equivalent to setting.

$$[\hat{p}(\kappa_o x_1/|\mathbf{x}|, \kappa_0 x_3/|\mathbf{x}|)] \approx [\hat{p}(0, 0)] = \frac{1}{(2\pi)^2} \int_{-\infty}^{\infty} dy_3 \int_{-\infty}^{0} [p(y_1, y_3)] dy_1 \equiv \frac{F(\omega)}{(2\pi)^2},$$

in equation (14), where $F(\omega)$ is the net normal force exerted on the fluid by the half-plane. This force may be determined exactly from the solution (6) to be given by

$$F(\omega) = -2\pi\mathrm{i}\int_{-\infty}^{\infty} \frac{p_s(k_1,0,\omega)\sqrt{\kappa_o + k_1}}{\sqrt{\kappa_o}(k_1 - \mathrm{i}0)}\,\mathrm{d}k_1. \tag{16}$$

It is unbounded in the incompressible limit in which $\kappa_o \to 0$, and cannot be reliably computed at low Mach numbers by a numerical simulation of the flow, being determined by the unsteady surface pressures over a distance from the edge of the order of the acoustic wavelength.

A correct prediction of the edge noise from Curle's formula is possible only when the surface pressures are known within the acoustic domain. To use equation (14), $[\hat{p}(\kappa_o x_1/|\mathbf{x}|, \kappa_o x_3/|\mathbf{x}|)|)]$ must be evaluated from the exact formula (6), in the form

$$\left[\hat{p}\left(\frac{\kappa_o x_1}{|\mathbf{x}|}, \frac{\kappa_o x_3}{|\mathbf{x}|}\right)\right] = \frac{-1}{2\sqrt{2\kappa_o}\,\pi\mathrm{i}\sin^{1/2}\psi\cos(\theta/2)} \times \int_{-\infty}^{\infty} \frac{\sqrt{\kappa_o \sin\psi + k_1}}{(\kappa_o x_1/|\mathbf{x}| - k_1)}\, p_s(k_1, \kappa_0 x_3/|\mathbf{x}|, \omega)\,\mathrm{d}k_1, \tag{17}$$

whose use in equation (14) leads directly to equation (8).

2.3. KIRCHHOFF INTEGRAL REPRESENTATION

The scattered pressure $p'(\mathbf{x}, \omega)$ of section 2.1. satisfies the Helmholtz equation (4) everywhere. By introducing a Green's function $G(\mathbf{x}, \mathbf{y}, \omega)$, which is *any* solution of

$$(\nabla^2 + \kappa_o^2)G = \delta(\mathbf{x} - \mathbf{y}) \tag{18}$$

with *outgoing* wave behaviour, $p'(\mathbf{x}, \omega)$ may be represented by the following Kirchhoff integral over S [24]:

$$p'(\mathbf{x}, \omega) = \oint_{\mathrm{S}} \left(G(\mathbf{x}, \mathbf{y}, \omega)\frac{\partial p'}{\partial y_n}(\mathbf{y}, \omega) - p'(\mathbf{y}, \omega)\frac{\partial G}{\partial y_n}(\mathbf{x}, \mathbf{y}, \omega)\right)\mathrm{d}S(\mathbf{y}), \tag{19}$$

where the normal derivatives $\partial/\partial y_n$ are directed into the fluid. This equation determines the scattered sound provided p' and $\partial p'/\partial y_n$ are known on S. However, for an arbitrary choice of the Green's function $G(\mathbf{x}, \mathbf{y}, \omega)$, and for the reasons discussed above for Curle's equation, acceptable predictions of the sound are possible only if the variations of p' and $\partial p'/\partial y_n$ on S are specified correctly over length scales comparable to the acoustic wavelengths.

For example, one might attempt to express the radiation entirely in terms of the surface pressure (already determined, say, by means of a subsidiary calculation

valid in the neighborhood of the edge) by using a "pressure release" Green's function that vanishes on S. The first term in the integrand of equation (19) is then absent, and $p'(\mathbf{x},\omega) = -\oint_S p'(\mathbf{y},\omega)\ \partial G(\mathbf{x},\mathbf{y},\omega)/\partial y_n\, \mathrm{d}S(\mathbf{y})$ would be an *exact* representation of the sound. But if $p'(\mathbf{y},\omega)$ in the integrand is known only in an incompressible approximation, the predicted behaviour of $p'(\mathbf{x},\omega)$ at large distances from the edge would be governed by the behavior of $G(\mathbf{x},\mathbf{y},\omega)$ as $|\mathbf{x}| \to \infty$, and the farfield scattered pressure would therefore be predicted to *vanish* on S, whereas for a rigid surface $|p'(\mathbf{x},\omega)|$ actually assumes its largest values there! In order for this latter behavior to be predicted, sufficient *phase* information characterizing changes in $p'(\mathbf{y},\omega)$ on S over distances of the order of the acoustic wavelength, must be included to ensure that a correct estimate is obtained for the asymptotic behavior of the integral (19) as $|\mathbf{x}| \to \infty$**.** This requirement is equivalent to the correction of the free field *dipole* directivity ($\cos\Theta \equiv \sin\psi \sin\theta$) of equation (14) brought about by the use of the exact formula (17) for $[p]$ in equation (12).

The need for such detailed phase information in the prescribed boundary values of p' and $\partial p'/\partial y_n$ can be avoided by using a Green's function that already satisfies the relevant boundary conditions on S. It can then be expected that surface values calculated from an incompressible model of the flow will be sufficient to determine the farfield sound at low Mach numbers. For the rigid half-plane the Green's function should have vanishing normal derivative on S (reciprocity actually implies that $\partial G/\partial x_n = 0$, $\partial G/\partial y_n = 0$ respectively on $x_1 < 0$, $x_2 = 0$ and $y_1 < 0$, $y_2 = 0$). Then the second term in the integrand of equation (19) is absent, and condition (3) gives

$$p'(\mathbf{x},\omega) = -\oint_{\mathrm{S}} \frac{\partial p_{\mathrm{I}}}{\partial y_n}(y_1,0,y_3,\omega)\, G(\mathbf{x},\mathbf{y};\omega)\, \mathrm{dS}(\mathbf{y}).$$

$$= -\int_{-\infty}^{\infty} \mathrm{d}y_3 \int_{-\infty}^{0} \frac{\partial p_{\mathrm{I}}}{\partial y_2}(y_1,0,y_3,\omega)\, [G(\mathbf{x},\mathbf{y},\omega)]\, \mathrm{d}y_1, \quad (20)$$

where

$$[G(\mathbf{x},\mathbf{y},\omega)] = G(\mathbf{x}, y_1, +0, y_3,\omega) - G(\mathbf{x}, y_1, -0, y_3,\omega) \quad (21)$$

is the jump in the value of G across the half-plane.

The integrals in equation (20) may be evaluated by taking $\partial p_{\mathrm{I}}/\partial y_2$ to have its value when compressibility is ignored, provided that those turbulence eddies responsible for the edge noise are always very much closer than an acoustic wavelength from the edge, which is always the case at sufficiently small Mach numbers. It then becomes appropriate to expand Green's function in terms of the non-dimensional source distance $\kappa_o\sqrt{y_1^2 + y_2^2}$ ($\sim \sqrt{y_1^2 + y_2^2}$/acoustic wavelength) from the edge. When the observation point $\mathbf{x}$ is in the acoustic far field we find [25]

$$G(\mathbf{x},\mathbf{y},\omega) = G_0(\mathbf{x},\mathbf{y},\omega) + G_1(\mathbf{x},\mathbf{y},\omega) + \cdots, \quad (22)$$

where, for $|\mathbf{x} - y_3\mathbf{i}_3| \to \infty$ and $\kappa_o\sqrt{y_1^2 + y_2^2} \ll 1$,

$$G_0(\mathbf{x}, \mathbf{y}, \omega) = \frac{-1}{4\pi|\mathbf{x} - y_3\mathbf{i}_3|} e^{i\kappa_o|\mathbf{x} - y_3\mathbf{i}_3|}, \quad G_1(\mathbf{x}, \mathbf{y}, \omega) = \frac{-1}{\pi\sqrt{2\pi i}} \frac{\sqrt{\kappa_o}\varphi^*(\mathbf{x})\varphi^*(\mathbf{y})}{|\mathbf{x} - y_3\mathbf{i}_3|^{3/2}} e^{i\kappa_o|\mathbf{x} - y_3\mathbf{i}_3|}, \tag{23}$$

in which $\mathbf{i}_3$ is a unit vector parallel to the x_3-axis (the edge), and the function

$$\varphi^*(\mathbf{x}) = \sqrt{r}\sin(\theta/2) \equiv \sqrt{|\mathbf{x}|}\sin^{1/2}\psi \sin(\theta/2) \tag{24}$$

is equivalent to the velocity potential of incompressible flow around the edge (in the anticlockwise direction) expressed in terms of polar co-ordinates $(x_1, x_2) = r(\cos\theta, \sin\theta)$. The component G_0 represents the radiation from a point source at $\mathbf{y}$ when scattering by the half-plane is neglected. The component G_1 provides the first correction due to the presence of the half-plane, and (since $[G_0] \equiv 0$) gives the leading approximation to the edge noise when used in equation (20).

By introducing the representation (5) of p_I in terms of the blocked pressure, we find, using equation (23) in equation (20),

$$\begin{aligned} p'(\mathbf{x}, \omega) &\approx \frac{\sqrt{2\kappa_o}\sin^{1/2}\psi \sin(\theta/2) e^{i\kappa_o|\mathbf{x}|}}{\pi\sqrt{\pi i}\,|\mathbf{x}|} \int_{-\infty}^{\infty} dy_3 \int_{-\infty}^{0} |y_1|^{1/2} \frac{\partial p_1}{\partial y_2}(y_1, 0, y_3)\, dy_3 \\ &= \frac{-\sqrt{i\kappa_o}\sin^{1/2}\psi \sin(\theta/2) e^{i\kappa_o|\mathbf{x}|}}{\pi\sqrt{2\pi}\,|\mathbf{x}|} \int_{-\infty}^{\infty} \gamma(k) p_s(\mathbf{k}, \omega)\, d^2\mathbf{k} \\ &\quad \times \int_{-\infty}^{\infty} e^{ik_3 y_3} dy_3 \int_{-\infty}^{0} |y_1|^{1/2} e^{ik_1 y_1} dy_1. \end{aligned} \tag{25}$$

The y_3-integral equals $2\pi\delta(k_3)$; the y_1-integral must be treated as the Fourier transform of a generalized function [26], and evaluated by integration by parts, when it is found to be equal to

$$\frac{-1}{2|k_1|}\sqrt{\frac{\pi i}{k_1 + i0}}.$$

When compressible effects in the specification of the blocked pressure are neglected, it may be assumed that $\kappa_o \ll k_1$ for all relevant values of k_1 in the wavenumber integral. Then $\gamma(k) \to i|k_1|$ and equation (25) reduces to precisely the low Mach number approximation (9) obtained previously by diffraction theory.

3. ARBITRARY TRAILING EDGE GEOMETRY

3.1. VORTEX SOUND THEORY

The diffraction theory of section 2.1 is conveniently extended to an airfoil of finite thickness (Figure 2) by means of the theory of vortex sound [25], in which the total enthalpy B, rather than the pressure or density, is taken as the fundamental acoustic variable. When the mean flow Mach number is small enough that the convection of sound may be ignored, and when the mean fluid density is constant,

$$\left(\frac{1}{c_o^2}\frac{\partial^2}{\partial t^2} - \nabla^2\right)B = \operatorname{div}(\boldsymbol{\Omega} \wedge \mathbf{v}), \tag{26}$$

where $\boldsymbol{\Omega}(\mathbf{x}, t) = \operatorname{curl} \mathbf{v}$ is the vorticity. In those regions where the unsteady motion is irrotational ($\boldsymbol{\Omega} = \mathbf{0}$) yet still, perhaps, predominantly non-linear, it can be described by a velocity potential $\phi(\mathbf{x}, t)$, say, which satisfies $B = -\partial\phi/\partial t$. In the acoustic far field, the small amplitude pressure fluctuations are determined in terms of B by the linear relation

$$\frac{p'(\mathbf{x}, t)}{\rho_0} \approx -\frac{\partial\phi}{\partial t} \equiv B(\mathbf{x}, t). \tag{27}$$

Equation (26) relates fluctuations in B to the vorticity and velocity. The radiation condition requires the solution to have outgoing wave behavior, and for each Fourier component of frequency ω it can be expressed as the sum of a Kirchhoff integral representing a contribution from the surface S of the airfoil [as in equation (19)] plus the direct radiation from the vortex sources:

$$B(\mathbf{x}, \omega) = \oint_S \left(\frac{\partial B}{\partial y_n}(\mathbf{y}, \omega) G(\mathbf{x}, \mathbf{y}, \omega) - B(\mathbf{y}, \omega)\frac{\partial G}{\partial y_n}(\mathbf{x}, \mathbf{y}, \omega)\right) \mathrm{dS}(\mathbf{y})$$

$$- \int G(\mathbf{x}, \mathbf{y}, \omega)\,(\operatorname{div}(\boldsymbol{\Omega} \wedge \mathbf{v})(\mathbf{y}, \omega))\,\mathrm{d}^3\mathbf{y}, \tag{28}$$

where $G(\mathbf{x}, \mathbf{y}, \omega)$ is an outgoing solution of equation (18).

Let the Green function satisfy the rigid surface condition $\partial G/\partial y_n = 0$ on S, and use the divergence theorem to transform the volume integral in equation (28) as follows:

$$\int G \operatorname{div}(\boldsymbol{\Omega} \wedge \mathbf{v})\,\mathrm{d}^3\mathbf{y} = -\oint_S G(\boldsymbol{\Omega} \wedge \mathbf{v}) \cdot \mathbf{n}\,\mathrm{dS}(\mathbf{y}) - \int (\boldsymbol{\Omega} \wedge \mathbf{v}) \cdot \nabla G\,\mathrm{d}^3\mathbf{y},$$

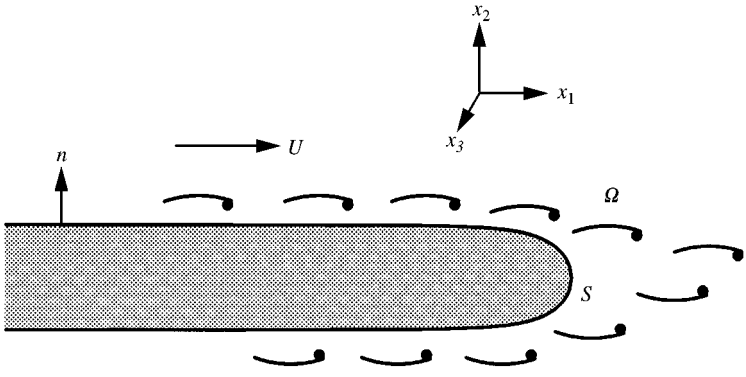

Figure 2. Low Mach number turbulent flow near the trailing edge of an airfoil of finite thickness.

where the unit normal $\mathbf{n}$ on S is directed into the fluid. Then

$$B(\mathbf{x},\omega)=\oint_{\mathrm{S}} G(\mathbf{x},\mathbf{y},\omega)\left(\frac{\partial B}{\partial y_n}+(\boldsymbol{\Omega}\wedge\mathbf{v})\cdot\mathbf{n}\right)(\mathbf{y},\omega)\,\mathrm{dS}(\mathbf{y})+\int\frac{\partial G}{\partial y}(\mathbf{x},\mathbf{y},\omega)\cdot(\boldsymbol{\Omega}\wedge\mathbf{v})(\mathbf{y},\omega)\,\mathrm{d}^3\mathbf{y}. \tag{29}$$

Very close to S viscous effects are dominated by shear stresses, and the momentum equation can be taken in Crocco's form,

$$\partial\mathbf{v}/\partial t+\nabla B=-\boldsymbol{\Omega}\wedge\mathbf{v}-\nu\,\mathrm{curl}\,\boldsymbol{\Omega},$$

where ν is the kinematic viscosity. But $\mathbf{v}\equiv\mathbf{0}$ on S when the airfoil is rigid and at rest. Hence equation (29) becomes

$$B(\mathbf{x},\omega)=\int\frac{\partial G}{\partial\mathbf{y}}(\mathbf{x},\mathbf{y},\omega)\cdot(\boldsymbol{\Omega}\wedge\mathbf{v})(\mathbf{y},\omega)\,\mathrm{d}^3\mathbf{y}-\nu\oint_{\mathrm{S}} G(\mathbf{x},\mathbf{y},\omega)\,\mathrm{curl}\,\boldsymbol{\Omega}\cdot\mathbf{n}\mathrm{dS}(\mathbf{y}),$$

and the identity $G\mathrm{curl}\,\boldsymbol{\Omega}\equiv\mathrm{curl}\,(G\boldsymbol{\Omega})+\boldsymbol{\Omega}\wedge\nabla G$ and the divergence theorem then yield

$$B(\mathbf{x},\omega)=\int\frac{\partial G}{\partial\mathbf{y}}(\mathbf{x},\mathbf{y},\omega)\cdot(\boldsymbol{\Omega}\wedge\mathbf{v})(\mathbf{y},\omega)\,\mathrm{d}^3\mathbf{y}-\nu\oint_{\mathrm{S}}\boldsymbol{\Omega}(\mathbf{y},\omega)\wedge\frac{\partial G}{\partial\mathbf{y}}(\mathbf{x},\mathbf{y},\omega)\cdot\mathbf{n}\mathrm{dS}(\mathbf{y}). \tag{30}$$

The surface integral is the contribution to the radiation from the unsteady skin friction on S, and is usually ignored when the Reynolds number is large.

The remaining integrals can be evaluated at low Mach numbers by expanding the Green function in the form (22), provided the characteristic acoustic wavelength

is much larger than the airfoil thickness. The principal contribution is from $G_1(\mathbf{x}, \mathbf{y}, \omega)$ which, however, must now be taken in the form [17]

$$G_1(\mathbf{x}, \mathbf{y}, \omega) = \frac{-1}{\pi\sqrt{2\pi \mathrm{i}}} \frac{\sqrt{\kappa_o}\varphi^*(\mathbf{x})\Phi^*(\mathbf{y})}{|\mathbf{x} - y_3\mathbf{i}_3|^{3/2}} \mathrm{e}^{\mathrm{i}\kappa_o|\mathbf{x} - y_3\mathbf{i}_3|}, \tag{31}$$

where the potential $\varphi^*(\mathbf{y}) \equiv \varphi^*(y_1, y_2)$ of equation (23) is replaced by $\Phi^*(y) = \Phi^*(y_1, y_2, y_3)$, which describes incompressible potential flow around the edge of the airfoil, such that

$$\Phi^*(y_1, y_2, y_3) \to \varphi^*(y_1, y_2) \quad \text{as } \sqrt{y_1^2 + y_2^2} \to \infty.$$

We now find, in the acoustic far field,

$$p'(\mathbf{x}, \omega) \approx \frac{-\rho_o \kappa_o^{1/2} \sin^{1/2}\psi \sin(\theta/2) \mathrm{e}^{\mathrm{i}\kappa_o|\mathbf{x}|}}{\pi\sqrt{2\pi \mathrm{i}}\,|\mathbf{x}|} \left\{ \int \frac{\partial \Phi^*(\mathbf{y})}{\partial \mathbf{y}} \cdot (\boldsymbol{\Omega} \wedge \mathbf{v})(\mathbf{y}, \omega)\, \mathrm{d}^3\mathbf{y} \right.$$

$$\left. - v \oint_S \boldsymbol{\Omega}(\mathbf{y}, \omega) \wedge \frac{\partial \Phi^*(\mathbf{y})}{\partial \mathbf{y}} \cdot \mathbf{n}\, \mathrm{dS}(\mathbf{y}) \right\}, \quad |\mathbf{x}| \to \infty. \tag{32}$$

The radiated sound automatically satisfies the rigid surface boundary condition on the distant parts of the airfoil, so that the vorticity $\boldsymbol{\Omega}$ and the velocity $\mathbf{v}$ in the integrands can be approximated by their values calculated for incompressible flow near the edge of the airfoil. The term in the brace brackets of equation (32) is proportional to the net normal force $F(\omega)$ exerted on the fluid by the airfoil. As noted in section 2.2, this force increases in proportion to the square root of the acoustic wavelength; in the present notation it is given by [17]

$$F(\omega) \approx 2\rho_o \sqrt{\frac{\mathrm{i}}{\pi\kappa_o}} \left\{ \int \frac{\partial \Phi^*(\mathbf{y})}{\partial \mathbf{y}} \cdot (\boldsymbol{\Omega} \wedge \mathbf{v})(\mathbf{y}, \omega)\, \mathrm{d}^3\mathbf{y} - \mathbf{v} \oint_S \boldsymbol{\Omega}(\mathbf{y}, \omega) \wedge \frac{\partial \Phi^*(\mathbf{y})}{\partial \mathbf{y}} \cdot \mathbf{n}\, \mathrm{dS}(\mathbf{y}) \right\}.$$

3.2. DIFFRACTION THEORY

The evaluation of equation (32) requires the vorticity and velocity fields to be known in the neighborhood of the edge. An alternative representation of the sound, which is analogous to equation (9) for the flat-plate airfoil, can be derived by consideration of the diffraction theory of section 2.1. We shall not, however, assume the boundary layer turbulence to be frozen during convection past the edge, but will introduce an "incident" disturbance B_I which is defined to be the exact solution of equation (26) *in the absence of the airfoil* when the vorticity $\boldsymbol{\Omega}$ and velocity $\mathbf{v}$ on the right-hand side of equation (26) have their exact values.

To calculate B_I, the interior of the airfoil is imagined to be replaced by fluid with no acoustic sources, wherein the actual motion is determined by the source

distribution $\boldsymbol{\Omega} \wedge \mathbf{v}$ outside S. Then for each component of frequency ω,

$$B_{\mathrm{I}}(\mathbf{x}, \omega) = \frac{1}{4\pi} \int_V \frac{\mathrm{e}^{\mathrm{i}\kappa_o|\mathbf{x}-\mathbf{y}|}}{|\mathbf{x}-\mathbf{y}|} \frac{\partial}{\partial \mathbf{y}} \cdot (\boldsymbol{\Omega} \wedge \mathbf{v})(\mathbf{y}, \omega)\, \mathrm{d}^3\mathbf{y}, \tag{33}$$

where V is the fluid volume outside S. When compressibility is neglected in the source region near the edge,

$$\frac{\partial}{\partial \mathbf{y}} \cdot (\boldsymbol{\Omega} \wedge \mathbf{v}) \equiv \frac{\partial^2 v_i v_j}{\partial y_i \partial y_j} - \nabla^2 \left(\frac{1}{2} v^2 \right), \tag{34}$$

and therefore, because $\mathbf{v}$ vanishes on S, the acoustic pressure $p_{\mathrm{I}} \approx \rho_o B_{\mathrm{I}}$ in the far field corresponds to the quadrupole field

$$p_{\mathrm{I}}(\mathbf{x}, \omega) \approx \frac{-\kappa_o^2 \mathrm{e}^{\mathrm{i}\kappa_o|\mathbf{x}|}}{4\pi|\mathbf{x}|} \left(\frac{x_i x_j}{|\mathbf{x}|^2} - \frac{1}{2}\delta_{ij} \right) \int_V \rho_o (v_i v_j)(\mathbf{y}, \omega)\, \mathrm{d}^3\mathbf{y}, \quad |\mathbf{x}| \to \infty, \tag{35}$$

which is negligible compared to the edge-generated sound.

The effect of the airfoil is calculated by setting

$$B(\mathbf{x}, t) = B'(\mathbf{x}, t) + B_{\mathrm{I}}(\mathbf{x}, t), \tag{36}$$

where B' satisfies the *homogeneous* form of equation (26) (no sources). B' and B_{I} are related by the no-slip boundary condition on S, which the momentum equation gives in the form

$$\nabla B' + \nabla B_{\mathrm{I}} = -\nu \operatorname{curl} \boldsymbol{\Omega} \quad \text{on S.} \tag{37}$$

Thus, when Kirchhoff's formula (19) is used (with p' replaced by B'), we find

$$B'(\mathbf{x}, \omega) = -\oint_{\mathrm{S}} G(\mathbf{x}, \mathbf{y}, \omega) \left(\frac{\partial B_{\mathrm{I}}}{\partial y_n} + \nu \operatorname{curl} \boldsymbol{\Omega} \cdot \mathbf{n} \right)(\mathbf{y}, \omega)\, \mathrm{dS}(\mathbf{y}), \tag{38}$$

provided $\partial G/\partial y_n = 0$ on S.

Taking the low Mach number expansion of the Green's function, the leading-order term of which is given by equation (31), we find

$$p'(\mathbf{x}, \omega) \approx \frac{\rho_o \kappa_o^{1/2} \sin^{1/2}\psi \sin(\theta/2)\, \mathrm{e}^{\mathrm{i}\kappa_o|\mathbf{x}|}}{\pi\sqrt{2\pi\mathrm{i}}\,|\mathbf{x}|}$$

$$\times \int_{\mathrm{S}} \left(\Phi^*(\mathbf{y}) \frac{\partial B_{\mathrm{I}}}{\partial y_n}(\mathbf{y}, \omega) + \nu \boldsymbol{\Omega}(\mathbf{y}, \omega) \wedge \frac{\partial \Phi^*(\mathbf{y})}{\partial \mathbf{y}} \cdot \mathbf{n} \right) \mathrm{dS}(\mathbf{y}), \quad |\mathbf{x}| \to \infty, \tag{39}$$

where the integrand is to be evaluated using incompressible approximations for $\partial B_1/\partial y_n$ and $\boldsymbol{\Omega}$.

This prediction of the far-field sound is identical to that given by equation (32). Indeed, because $\partial \Phi^*/\partial y_n = 0$ on S, the following relations are readily seen to transform the first term of the integral of equation (39) into the corresponding term in equation (32):

$$\operatorname{div}(\Phi^* \nabla B_\mathrm{I} - B_\mathrm{I} \nabla \Phi^*) \equiv \Phi^* \nabla^2 B_\mathrm{I} - B_\mathrm{I} \nabla^2 \Phi^* \equiv \Phi^* \nabla^2 B_\mathrm{I} \approx -\Phi^* \operatorname{div}(\boldsymbol{\Omega} \wedge \mathbf{v}),$$

where the final approximation follows from the incompressible limit of equation (26).

By setting $\kappa_o = 0$ in equation (33) we derive a local incompressible representation of B_I, from which it is readily deduced that

$$\nabla B_\mathrm{I} + \boldsymbol{\Omega} \wedge \mathbf{v} = \operatorname{curl} \int_V \frac{\operatorname{curl}(\boldsymbol{\Omega} \wedge \mathbf{v})\, \mathrm{d}^3\mathbf{y}}{4\pi|\mathbf{x}-\mathbf{y}|} \equiv -\operatorname{curl} \int_V \left(\frac{\partial \boldsymbol{\Omega}}{\partial t} - \nu \nabla^2 \boldsymbol{\Omega} \right) \frac{\mathrm{d}^3\mathbf{y}}{4\pi|\mathbf{x}-\mathbf{y}|}, \tag{40}$$

where use has been made of the curl of the incompressible momentum equation $\partial \mathbf{v}/\partial t + \nabla \mathrm{B} = -\boldsymbol{\Omega} \wedge \mathbf{v} - \nu \operatorname{curl} \boldsymbol{\Omega}$. In the viscous sublayer, close to the surface of the airfoil, the motion becomes *linear* and

$$\partial \boldsymbol{\Omega}/\partial t - \nu \nabla^2 \boldsymbol{\Omega} \approx \mathbf{0}.$$

Outside the sublayer viscous diffusion is negligible, and $\nu \nabla^2 \boldsymbol{\Omega}$ may be discarded from the integrand. Hence, we can introduce an "upwash velocity" $\mathbf{v}_\mathrm{I}$ by means of the Biot–Savart formula [27],

$$\mathbf{v}_\mathrm{I}(\mathbf{x}, t) = \operatorname{curl} \int_{V_\delta} \frac{\boldsymbol{\Omega}(\mathbf{y}, t)\, \mathrm{d}^3\mathbf{y}}{4\pi|\mathbf{x}-\mathbf{y}|}, \tag{41}$$

where the integration is confined to the boundary layer vorticity in the non-linear region V_δ *outside* the viscous sublayer. On S and within the volume of the airfoil, $\partial \mathbf{v}_\mathrm{I}/\partial t = -\nabla B_\mathrm{I}$, in terms of which the far-field sound becomes

$$p'(\mathbf{x}, \omega) \approx \frac{\rho_o \omega \sqrt{\mathrm{i}\kappa_o}\, \sin^{1/2}\psi \sin(\theta/2)\, \mathrm{e}^{\mathrm{i}\kappa_o|\mathbf{x}|}}{\pi\sqrt{2\pi}\,|\mathbf{x}|} \oint_\mathrm{S} \Phi^*(\mathbf{y})\, v_{\mathrm{I}n}(\mathbf{y}, \omega)\, \mathrm{dS}(\mathbf{y}), \quad |\mathbf{x}| \to \infty, \tag{42}$$

where $v_{\mathrm{I}n} = \mathbf{v}_\mathrm{I} \cdot \mathbf{n}$. Note that in applications to problems in which, for the purpose of calculation, the whole motion is regarded as inviscid, definition (41) makes it clear that in calculating $\mathbf{v}_\mathrm{I}$ the *bound vorticity* on S must be excluded from the integral.

Equation (42) generalizes the Chase–Chandiramani formula (9) for the flat-plate airfoil, to which it reduces when S is a semi-infinite half-plane. To see this it is

necessary to note that, in an incompressible approximation of the flow near the edge, the incident pressure $p_{\rm I}$ of equation (5) is the solution of

$$\nabla^2 p_{\rm I} = -\rho_0 \frac{\partial^2 v_i v_j}{\partial x_i \partial x_j} \equiv -\rho_o \,\mathrm{div}\,(\boldsymbol{\Omega} \wedge \mathbf{v}) - \rho_o \nabla^2 \left(\frac{1}{2} v^2\right)$$

when the presence of the airfoil is ignored. Hence $B_{\rm I} = p_{\rm I}/\rho_o + \frac{1}{2} v^2$, where $\mathbf{v}$ is the fluid velocity, which vanishes on and within S where, accordingly,

$$\frac{\partial \mathbf{v}_{\rm I}}{\partial t} = -\nabla B_{\rm I} \equiv \frac{-1}{\rho_o} \nabla p_{\rm I}. \tag{43}$$

When $v_{{\rm I}n}$ in equation (41) is replaced by $(1/{\rm i}\rho_o\omega)\,\partial p_{\rm I}/\partial y_n$ the first line of equation (25) is recovered, leading to our previous result (9).

For a time-stationary random flow past the edge we can introduce a frequency correlation function $\mathscr{R}_{vv}(\mathbf{y}, \mathbf{y}', \omega)$ that satisfies

$$\langle v_{{\rm I}n}(\mathbf{y}, \omega)\, v^*_{{\rm I}n}(\mathbf{y}', \omega')\rangle = \mathscr{R}_{vv}(\mathbf{y}, \mathbf{y}', \omega)\, \delta(\omega - \omega'). \tag{44}$$

The acoustic pressure frequency spectrum [defined as for equation (11)] then becomes

$$\Phi(\mathbf{x}, \omega) \approx \frac{\rho_o^2 \omega^3 \sin\psi \sin^2(\theta/2)}{\pi^3 c_o |\mathbf{x}|^2} \oint_{\rm S} \mathscr{R}_{vv}(\mathbf{y}, \mathbf{y}', \omega) \Phi^*(\mathbf{y})\, \Phi^*(\mathbf{y}')\, {\rm dS}(\mathbf{y})\, {\rm dS}(\mathbf{y}'), \quad \omega > 0. \tag{45}$$

3.3. TWO-DIMENSIONAL SOURCE DISTRIBUTIONS

We record here the modifications of formulae given above when the aeroacoustic sources and trailing edge can be regarded as two-dimensional, with no dependence on the spanwise coordinate x_3. At very small Mach numbers, the dominant component of the Green's function whose normal derivative vanishes on S is obtained by integrating equation (31) over $-\infty < y_3 < \infty$. When $\mathbf{x}$ lies in the acoustic far field the integration can be performed by the method of stationary phase, which yields [5]

$$G_1(\mathbf{x}, \mathbf{y}, \omega) \approx -\frac{\varphi^*(\mathbf{x}) \Phi^*(\mathbf{y})}{\pi |\mathbf{x}|} \,{\rm e}^{{\rm i}\kappa_o |\mathbf{x}|} \equiv \frac{-\sin(\theta/2) \Phi^*(\mathbf{y})}{\pi |\mathbf{x}|^{1/2}} \,{\rm e}^{{\rm i}\kappa_o |\mathbf{x}|}, \tag{46}$$

where now $\mathbf{x} = (x_1, x_2)$, $\mathbf{y} = (y_1, y_2)$.

Thus, the two-dimensional analog of equation (32) is the *cylindrically spreading* wave field

$$p'(\mathbf{x},\omega) \approx \frac{-\rho_o \sin(\theta/2)\, e^{ik_o|\mathbf{x}|}}{\pi|\mathbf{x}|^{1/2}} \left\{ \int \frac{\partial \Phi^*(\mathbf{y})}{\partial \mathbf{y}} \cdot (\boldsymbol{\Omega} \wedge \mathbf{v})(\mathbf{y},\omega)\, d^2\mathbf{y} \right.$$

$$\left. - v \oint_S \boldsymbol{\Omega}(\mathbf{y},\omega) \wedge \frac{\partial \Phi^*(\mathbf{y})}{\partial \mathbf{y}} \cdot \mathbf{n}\, ds(\mathbf{y}) \right\}, \quad |\mathbf{x}| \to \infty,$$

where $ds > 0$ is the line element on the airfoil profile in the x_1x_2-plane. This has the simple time-domain form

$$p'(\mathbf{x},t) \approx \frac{-\rho_o \sin(\theta/2)}{\pi|\mathbf{x}|^{1/2}} \left[\int \frac{\partial \Phi^*(\mathbf{y})}{\partial \mathbf{y}} \cdot (\boldsymbol{\Omega} \wedge \mathbf{v})(\mathbf{y},t)\, d^2\mathbf{y} - v \oint_S \boldsymbol{\Omega}(\mathbf{y},t) \wedge \frac{\partial \Phi^*(\mathbf{y})}{\partial \mathbf{y}} \cdot \mathbf{n}\, ds(\mathbf{y}) \right],$$

which decays in amplitude like $1/|\mathbf{x}|^{1/2}$ at the large distances from the edge, and where the term in the square brackets [ ] is evaluated at the retarded time $t - |\mathbf{x}|/c_o$. For inviscid (or very high Reynolds number) flow we can take

$$p'(\mathbf{x},t) \approx \frac{-\rho_o \sin(\theta/2)}{\pi|\mathbf{x}|^{1/2}} \left[\int \frac{\partial \Phi^*(\mathbf{y})}{\partial \mathbf{y}} \cdot (\boldsymbol{\Omega} \wedge \mathbf{v})(\mathbf{y},t)\, d^2\mathbf{y} \right]. \tag{47}$$

Similarly, the diffraction theory formulae (38) and (42) have the corresponding representations

$$p'(\mathbf{x},t) \approx \frac{\rho_o \sin(\theta/2)}{\pi|\mathbf{x}|^{1/2}} \oint_S \Phi^*(\mathbf{y}) \left[\frac{\partial B_I}{\partial y_n}(\mathbf{y},t) \right] ds$$

$$\equiv -\frac{\rho_o \sin(\theta/2)}{\pi|\mathbf{x}|^{1/2}} \oint_S \Phi^*(\mathbf{y}) \left[\frac{\partial v_{In}}{\partial t}(\mathbf{y},t) \right] ds, \quad |\mathbf{x}| \to \infty, \tag{48}$$

where the skin friction contribution has been discarded.

4. ROUNDED TRAILING EDGE

Rounded or bevelled trailing edges, of the type depicted in Figure 3(a), are frequently used in experimental studies of trailing edge noise at low Mach numbers [1, 28, 29]. The simplified geometry is suitable for validating numerical methods for edge noise prediction. When the Mach number is small enough for the edge flow to be regarded as incompressible, it is necessary to be able to determine numerically the velocity and vorticity distribution near the edge, or equivalently, the "upwash" velocity v_{In}. In this section the procedure is illustrated for a highly simplified two-dimensional edge flow that can be treated analytically.

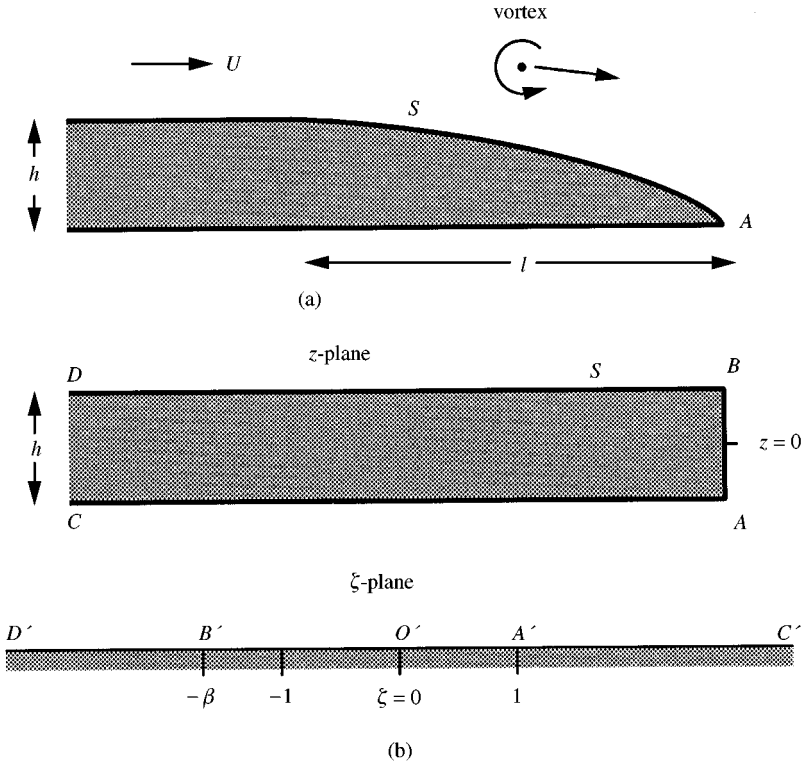

Figure 3. (a)Airfoil of thickness h with a rounded trailing edge section of length l. (b) Mapping the region outside a rectangular airfoil onto the upper-half of the ζ-plane.

4.1. FORMULATION

A line (or "point") vortex of circulation Γ is parallel to the edge of the airfoil and convects in the mean flow. Except very close to the edge, the airfoil has uniform thickness h and its "upper" and "lower" surfaces coincide with the planes $x_2 = \pm \frac{1}{2}h$. The upper surface is rounded over the interval $-l < x_1 < 0$, and meets the lower surface at A: $x_1 = 0$, $x_2 = -\frac{1}{2}h$ [Figure 3(a)]. At large distances from the airfoil the mean flow is at speed U in the x_1-direction, and the mean circulation around the airfoil is assumed to be adjusted to make A a stagnation point.

Viscosity is ignored in the body of the fluid, so that the two-dimensional motion of the vortex can be determined by mapping the fluid region bounded by the airfoil in the complex plane of $z = x_1 + \mathrm{i}x_2$ onto the upper-half of the ζ-plane. To do this we introduce the complex function

$$f(\zeta, \beta) = -\frac{4}{\pi(1+\beta)^2}\left(\zeta + \frac{\beta - 1}{2}\right)\sqrt{\zeta + \beta}\,\sqrt{\zeta - 1} + \frac{1}{\pi}\ln\left[\left(\zeta + \frac{\beta - 1}{2}\right) + \sqrt{\zeta + \beta}\sqrt{\zeta - 1}\right] - \frac{\mathrm{i}}{2} - \frac{1}{\pi}\ln\left(\frac{1+\beta}{2}\right), \quad \beta = \text{constant} > -1. \tag{49}$$

The transformation

$$z/h = f(\zeta, \beta)$$

maps the exterior of the semi-infinite airfoil of uniform *rectangular* cross-section and thickness h shown in Figure 3(b) onto $\mathrm{Im}\,\zeta > 0$, such that the boundary points C, A, B, D on S correspond respectively to the points C′, A′, B′, D′ on the real ζ-axis.

It may then be verified that the composite transformation

$$\frac{z}{h} = \frac{1}{(1+\alpha)}\,[f(\zeta, 1) + \alpha f(\zeta, \beta)], \quad \alpha > 0, \quad \beta > +1, \tag{50}$$

where α is a second constant, maps the real ζ-axis onto an airfoil profile S whose upper and lower surfaces coincide with $x_2 = \pm \frac{1}{2}h$ respectively for $\mathrm{Re}\,\zeta < -\beta$ and $\mathrm{Re}\,\zeta > 1$. The interval $-\beta < \mathrm{Re}\,\zeta < -1$ maps into an upper "rounded" section of the trailing edge [as in Figure 3(a)] which terminates at $\zeta = -1$ at the top of a vertical end-face $(x_1 = 0, \quad -\frac{1}{2}h < x_2 < -\frac{1}{2}h + \Delta)$ of thickness Δ, that corresponds to the interval $-1 < \mathrm{Re}\,\zeta < 1$. The constants α and β are determined by the prescribed values of the ratios l/h and Δ/h. For the calculations presented in this paper we take

$$\alpha = 600, \; \beta = 86.9370 \tag{51}$$

for which $l/h = 4$ and $\Delta/h = 0.0074$. The corresponding airfoil profile is that shown in Figure 3(a) (because $\Delta \ll h$ the end-face cannot be distinguished).

When the edge A is a stagnation point, the complex velocity potential of the mean flow is readily confirmed to be given by

$$w_m = \frac{-Uh}{\pi(1+\alpha)}\left[1 + \frac{4\alpha}{(1+\beta)^2}\right](\zeta - 1)^2, \tag{52}$$

which becomes asymptotically $w_m \approx Uz$ when $|z| \gg h$. The vortex Γ is convected by the mean flow and by the induced velocity field of "image" vortices in the airfoil. If A is also a stagnation point of the unsteady flow, i.e., if the unsteady Kutta condition is applied there, additional vorticity is shed from A, and will also influence the motion of Γ. We first consider the motion and sound generation in the absence of vortex shedding.

4.2. NO VORTEX SHEDDING

Let $z_o(t)$ denote the complex position of Γ at time t. The velocity potential of the (incompressible) flow produced by Γ is

$$w_\Gamma = \frac{-\mathrm{i}\Gamma}{2\pi}\,\{\ln(\zeta - \zeta_o) - \ln(\zeta - \zeta_o^*)\},$$

where $\zeta_o = \zeta(z_o)$ is the image of z_o in the ζ-plane, and the asterisk denotes complex conjugate. The complex potential of the velocity component of the motion of Γ produced by image vorticity is obtained by subtracting the "self-potential" $(-i\Gamma/2\pi)\ln(z - z_o)$ from w_Γ. The equation of motion of Γ is accordingly obtained in the form

$$\frac{\mathrm{d}z_o^*}{\mathrm{d}t} = \frac{-i\Gamma}{2\pi}\left[\frac{\zeta_o''}{2\zeta_o'} - \frac{\zeta_o'}{\zeta_o - \zeta_o^*}\right] + \left(\frac{\mathrm{d}w_m}{\mathrm{d}z}\right)_o, \tag{53}$$

where the suffix "o" implies evaluation at $z = z_o$, and the primes indicate differentiation with respect to z. This equation must be integrated numerically to determine the path of the vortex, and it is convenient to do this in the ζ-plane, where it is equivalent to

$$\frac{\mathrm{d}\zeta_o^*}{\mathrm{d}t} = \frac{-i\Gamma\zeta_o'^*}{2\pi}\left[\frac{\zeta_o''}{2\zeta_o'} - \frac{\zeta_o'}{\zeta_o - \zeta_o^*}\right] + \left(\frac{\mathrm{d}w_\mathrm{m}}{\mathrm{d}\zeta}\right)_o |\zeta_o'|^2. \tag{54}$$

The solid curve in Figure 4(a) depicts the calculated path when the vortex is released at a large distance upstream of the edge, above the airfoil at a stand-off distance $d = \frac{1}{2}h$ from the upper surface. The vortex initially translates along a path parallel to the upper flat surface of the airfoil at speed $U + u$, where

$$u = \Gamma/4\pi d. \tag{55}$$

The results discussed below are obtained for $u = -0.1U$. This corresponds roughly to a typical large fluctuation velocity close to the wall of a turbulent boundary layer [30]. The trajectory shown in Figure 4(a) was computed (using a fourth order Runge–Kutta scheme [20]) by adjusting the value of ζ_o far upstream of the edge to make the initial stand-off distance d (determined in terms of ζ_o by equation (50)] equal to $\frac{1}{2}h$. The vortex location is indicated in the figure at different non-dimensional times Ut/h, measured from the instant that it crosses $x_1 = 0$.

Two other trajectories are also shown in the figure. The "frozen" path corresponds to the Chase–Chandiramani approximation [11, 12], in which turbulent structures are assumed to translate past the edge at a uniform mean convection velocity parallel to the airfoil. The position of the vortex on this path has been calculated by taking the uniform convection velocity to be $U + u$ (not U), i.e., its "exact" value when located above the flat section of the surface of the airfoil. The path labelled "rdt" is determined by neglecting the influence of image vortices on the motion of Γ, whose equation of motion is now equation (53) with the omission of the first of the two terms on the right-hand side. This corresponds to the approximation of "rapid distortion theory", where each turbulent element is assumed to convect across an inhomogeneous region at the local mean stream velocity [31, 32]; for the purpose of this illustration it has again been assumed that the mean velocity far from the edge is $U + u$. In all cases, therefore, the vortex passes by the edge at approximately the same speed.

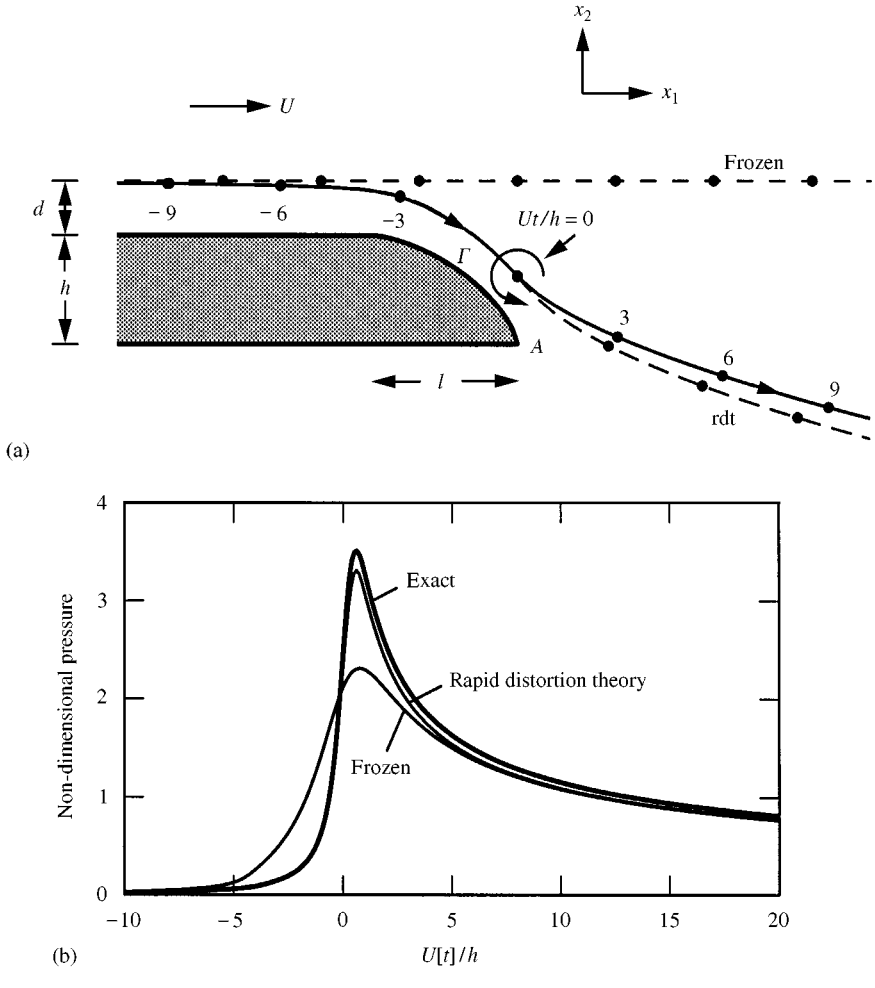

Figure 4. Trajectories of the vortex Γ past the trailing edge when $u = -0{\cdot}1U$, $l/h = 4$, $d/h = 0{\cdot}5$. (b) Acoustic pressure signatures $p/\{\rho_o(\Gamma/h)^2 \sin(\theta/2)\sqrt{h/|\pi\mathbf{x}|}/8\}$; $d/h = 0{\cdot}5$; $\kappa/U = -0{\cdot}1$.

Sound is generated by the vortex principally during its passage past the edge, and can be calculated from either of the formulae (47) or (48), by noting that the transformation (50) implies that

$$\Phi^*(\mathbf{y}) = \mathrm{Re}\left\{-\zeta\sqrt{\frac{h}{\pi(1+\alpha)}\left(1+\frac{4\alpha}{(1+\beta)^2}\right)}\right\}, \tag{56}$$

where ζ is the image of $z = y_1 + \mathrm{i}y_2$, and $\mathbf{y} = (y_1, y_2)$.

Now, for a line vortex,

$$\boldsymbol{\Omega} = \Gamma\mathbf{i}_3\,\delta(\mathbf{y} - \mathbf{x}_o(t)) \quad \text{and} \quad \mathbf{v} = \frac{\mathrm{d}\mathbf{x}_o}{\mathrm{d}t}(t), \tag{57}$$

where $\mathbf{x}_o(t)$ is the vortex location at time t calculated from equations (53) and (54), and we therefore find from equation (47),

$$p'(\mathbf{x}, t) \approx \frac{-\rho_o \Gamma \sin(\theta/2)}{\pi^{3/2}} \sqrt{\frac{h}{|\mathbf{x}|}} \left(\frac{1 + 4\alpha/(1+\beta)^2}{1+\alpha}\right)^{1/2} \quad \mathrm{lm}\left[\frac{\mathrm{d}\zeta_o}{\mathrm{d}t}\right], \quad |\mathbf{x}| \to \infty, \quad (58)$$

where ζ_o is evaluated at the retarded time $[t] = t - |\mathbf{x}|/c_o$.

The "exact" curve in Figure 4(b) is a non-dimensional representation of the pressure signature plotted against $U[t]/h$. Also shown are the corresponding predictions of rapid distortion theory and the frozen approximation. The high-frequency components of the sound are generated by scattering at the sharp edge of the airfoil, and the peak radiated pressure occurs in the neighborhood of $[t] = 0$ when the vortex passes close to the edge. In the frozen approximation the contributions to the sound at higher frequencies are reduced because small-scale disturbances generated by the vortex, that are responsible for the high-frequency sound, decay rapidly as the stand-off distance of the vortex path from the edge A increases.

The sound can also be calculated from the diffraction theory formula (48). To do this, recall that $B_{\mathrm{I}} = -\partial\phi_{\mathrm{I}}/\partial t$, where in two-dimensions the "free-space" velocity potential ϕ_{I} of the vortex is given by

$$\phi_{\mathrm{I}}(\mathbf{x}, t) = \mathrm{Re}\left\{\frac{-\mathrm{i}\Gamma}{2\pi} \ln(z - z_o(t))\right\}, \quad z = x_1 + \mathrm{i}x_2.$$

It now follows, using the representation (56) of $\Phi^*(\mathbf{y})$, that

$$p'(\mathbf{x}, t) \approx -\frac{\rho_o \Gamma \sin(\theta/2)}{2\pi^{5/2}} \sqrt{\frac{h}{|\mathbf{x}|}} \left(\frac{1 + 4\alpha/(1+\beta)^2}{1+\alpha}\right)^{1/2} \mathrm{Re}\left[\frac{\mathrm{d}z_o}{\mathrm{d}t} \oint_{\mathrm{S}} \frac{\zeta \mathrm{d}z}{(z - z_o)^2}\right], \quad |\mathbf{x}| \to \infty, \quad (59)$$

where the integration is in the *anticlockwise* direction about the contour S of the airfoil in the z-plane, and the square brackets denote evaluation at the retarded time $t - |\mathbf{x}|/c_o$.

The integrand $\sim \mathrm{O}(1/|z|^{3/2})$ as $|z| \to \infty$. The integral may therefore be evaluated by residues by shifting the integration contour to a large circle at infinity, thereby capturing a contribution from the pole at $z = z_o(t)$. This procedure yields equation (58). Alternatively, equation (59) can be used to investigate the contributions to the diffraction radiation from the lower and upper surfaces of the airfoil, which are determined by the respective contributions to the integral from the lower surface between $z = -\infty - \mathrm{i}h/2$ and $z = -\mathrm{i}h/2$ and from the upper, rounded surface between $z = -\mathrm{i}h/2$ and $-\infty + \mathrm{i}h/2$. These separate integrals have been evaluated numerically, and the corresponding pressures are labelled "lower surface" and "upper" in Figure 5 for the conditions of Figure 4, for the case in which the vortex

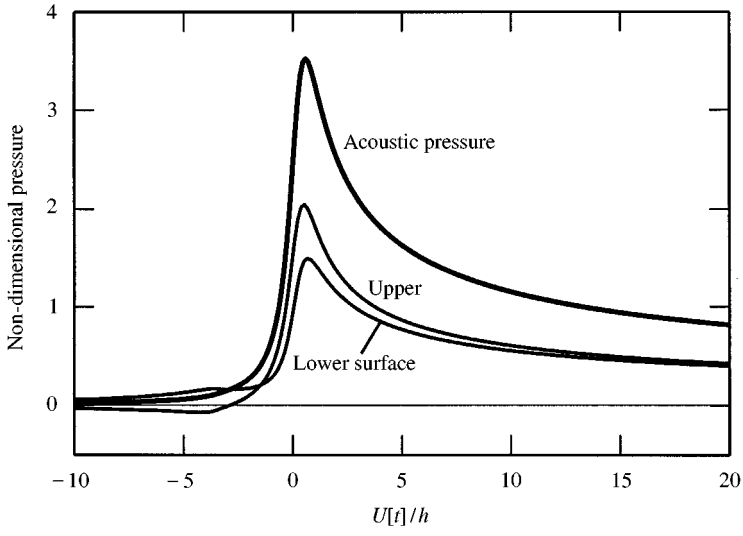

Figure 5. The acoustic pressure $p/\{\rho_o(\Gamma/h)^2 \sin(\theta/2)\sqrt{h/|\pi \mathbf{x}|}/8\}$ and the separate contributions from the upper and lower surfaces of the airfoil of Figure 4 when $u = -0{\cdot}1U$, $l/h = 4$, $d/h = 0{\cdot}5$ and when the vortex moves along the solid ("exact") trajectory of Figure 4(a).

moves along the solid ("exact") path of Figure 4(a). The net acoustic pressure is the algebraic sum of these separate contributions.

4.3. INFLUENCE OF VORTEX SHEDDING

When the Kutta condition is imposed at the edge A of the airfoil during the passage of Γ, vorticity is shed into the flow and swept downstream. The acoustic radiation consists of the direct sound generated by Γ, considered in section 4.2, and the sound generated by the wake. If $u \ll U$, where $u = \Gamma/4\pi d$ is the characteristic induced velocity of the vortex, the trajectory and the acoustic pressure signature of Γ are to a good approximation the same as when the vortex convects at the local mean stream velocity (according to 'rapid distortion theory", see Figure 4). We shall therefore adopt this approximation to examine the influence of the wake, by assuming that both Γ and the shed vorticity convect at the local free stream velocity along undisturbed streamlines of the mean flow. This is equivalent to the linearized approximation of unsteady thin airfoil theory [33, 34], where the airfoil is modelled as a plate of infinitesimal thickness parallel to the mean flow (as in section 2), and all perturbation quantities are proportional to the amplitude of an incident "gust". In that case, however, both the gust and the wake vorticity convect parallel to the plate at the same, uniform mean stream velocity, and the acoustic pressure generated by the wake turns out to be equal and opposite to that produced by the gust, so that there is no net radiation from the edge [4].

The shedding does not become significant until Γ is close to the edge. It will be modelled by releasing from the edge A a succession of elementary line vortices of

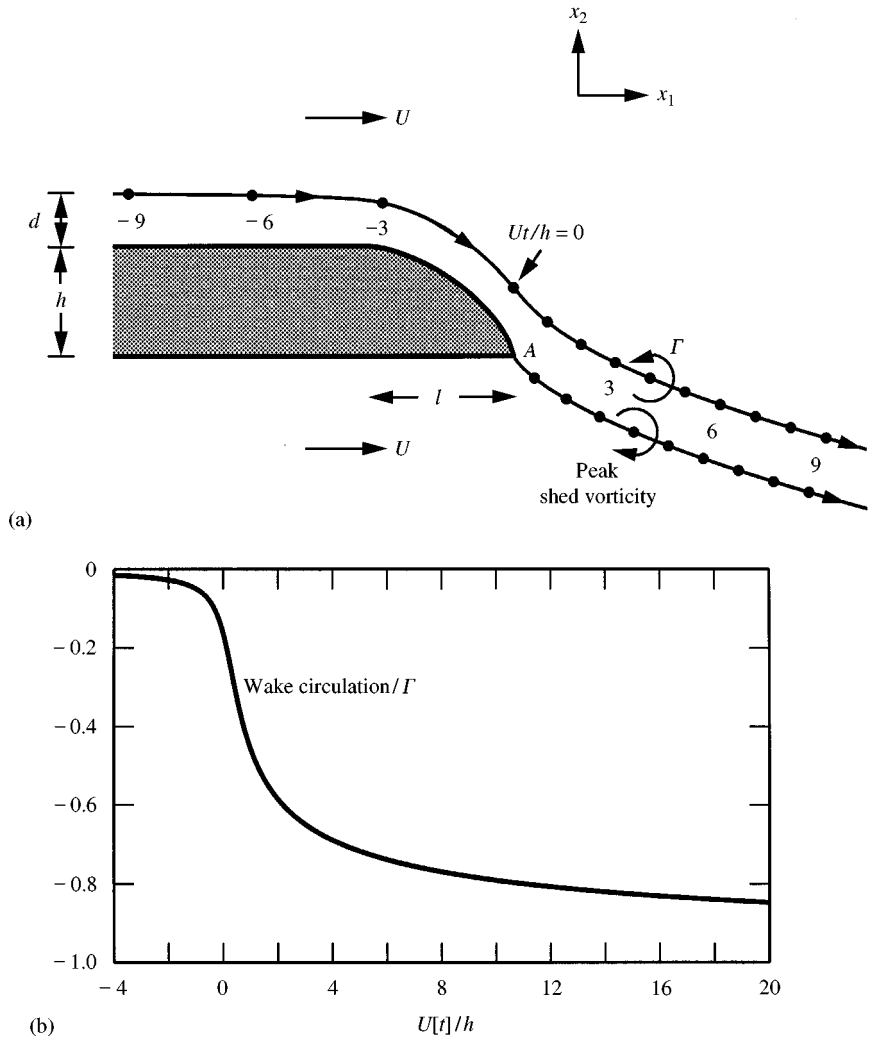

Figure 6. (a) Trajectories of the vortex Γ and shed vorticity in the approximation of rapid distortion theory for $u = -0{\cdot}1U$, $l/h = 4$, $d/h = 0{\cdot}5$. (b) Total wake circulation as a function of time.

circulation Γ_k at discrete times $t = t_k$, $k \geqslant 1$. Let z_k, ζ_k denote respectively the position of Γ_k in the z-plane and its image in the upper-half of the ζ-plane at time t. These vortices lie on the stagnation streamline emanating from A [see Figure 6(a)], along which they convect at the local mean velocity; their images ζ_k are located on the line $\mathrm{Re}\,\zeta = 1$ extending from the real axis into the upper half-plane. At time t_j, when there are j shed vortices in the flow, the complex potential of the *unsteady* component of the flow is

$$w = \frac{-\mathrm{i}\Gamma}{2\pi}\{\ln(\zeta - \zeta_o) - \ln(\zeta - \zeta_o^*)\} + \sum_{k=1}^{j} \frac{-\mathrm{i}\Gamma_k}{2\pi}\{\ln(\zeta - \zeta_k) - \ln(\zeta - \zeta_k^*)\}. \qquad (60)$$

The Kutta condition is satisfied at A by setting $\mathrm{d}w/\mathrm{d}\zeta = 0$ at $\zeta = 1$. This determines the strength Γ_j of the jth vortex in terms of Γ and all of the previously shed vortices according to

$$\Gamma_j = -\operatorname{Im}\zeta_j \left\{ \frac{\Gamma \operatorname{Im}\zeta_o}{|1-\zeta_o|^2} + \sum_{k=1}^{j-1} \frac{\Gamma_k}{\operatorname{Im}\zeta_k} \right\}. \tag{61}$$

To apply this formula it is necessary to specify the initial position $\zeta_j = 1 + \mathrm{i}\varepsilon$ of the jth vortex on the stagnation streamline $\operatorname{Re}\zeta = 1$, where ε is small and positive, whose precise value does not materially affect the results. At the next time step in the calculation all of the shed vortices will have moved along this streamline by distances determined by the mean velocity potential (52).

The results of such a calculation are illustrated in Figure 6(a), for the rounded airfoil considered previously. The initial stand-off distance d of Γ far upstream of the edge is equal to $\frac{1}{2}h$, as before, and the characteristic velocity u of equation (55) is again taken to be $-0{\cdot}1U$. The trajectories of the incident and shed vortices are the streamlines of the mean flow shown in Figure 6(a). Time is measured from the instant that Γ crosses $x_1 = 0$, and the figure shows the position of Γ at various times, and also the corresponding location of the peak shed vorticity. This peak is shed into the flow when Γ is close to the edge, and translates downstream with Γ on a parallel path at roughly the same velocity. Figure 6(b) indicates how the overall circulation of the wake vorticity is opposite in sign to Γ and has a final magnitude equal to about 80% of Γ. The slope of the wake circulation curve is always negative, showing that the sign of each elementary vortex Γ_j is always opposite to Γ.

The sound generated by the impinging vortex and the wake at the retarded time $t_j = t - |\mathbf{x}|/c_o$, just after the release of the jth vortex from A, can be calculated from either of the following generalizations of equations (58) and (59),

$$p'(\mathbf{x},t) \approx \frac{-\rho_o \sin(\theta/2)}{\pi^{3/2}} \sqrt{\frac{h}{|\mathbf{x}|}} \left(\frac{1 + 4\alpha/(1+\beta)^2}{1+\alpha} \right)^{1/2}$$

$$\times \begin{cases} \operatorname{Im}\left[\Gamma \frac{\mathrm{d}\zeta_o}{\mathrm{d}t} + \sum_{k=1}^{j} \Gamma_k \frac{\mathrm{d}\zeta_k}{\mathrm{d}t}\right], \\ \frac{1}{2\pi} \operatorname{Re}\left[\Gamma \frac{\mathrm{d}z_o}{\mathrm{d}t} \oint_S \frac{\zeta \mathrm{d}z}{(z-z_o)^2} + \sum_{k=1}^{j} \Gamma_k \frac{\mathrm{d}z_k}{\mathrm{d}t} \oint_S \frac{\zeta \mathrm{d}z}{(z-z_k)^2}\right], \end{cases} \qquad |\mathbf{x}| \to \infty\,. \tag{62}$$

The pressure signature is plotted against $U[t]/h$ in Figure 7. Also plotted are the separate contributions from Γ and from the wake, which are of comparable magnitudes, but opposite in sign. Because of the progressive increase in the total wake circulation, when $U[t]/h$ exceeds about 5 the separate acoustic pressures attributable to Γ and the wake are effectively equal and opposite. Thus, the net radiation is significantly different from zero only for retarded times $U[t]/h \sim \mathrm{O}(1)$ when Γ is very close to the sharp edge A. This may be contrasted with the analogous result for an airfoil of infinitesimal thickness [4], for which the predicted radiations from Γ and from the wake are equal and opposite for *all* times, and linear theory accordingly predicts that no sound is produced at the trailing edge.

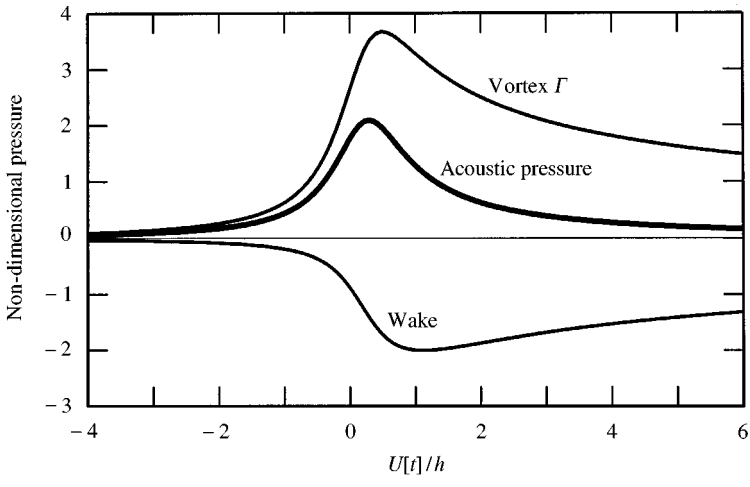

Figure 7. The acoustic pressure $p/\{\rho_o(\Gamma/h)^2 \sin(\theta/2)\sqrt{h/|\pi\mathbf{x}|}/8\}$ and the separate contributions from the vortex Γ and the vortex wake in the rapid distortion approximation of Figure 6, when $u = -0{\cdot}1U$, $l/h = 4$, $d/h = 0{\cdot}5$.

5. CONCLUSION

In this paper, the Chase–Chandiramani diffraction theory for estimating trailing edge noise from a flat plate, zero thickness airfoil has been extended to low Mach number flows past a non-compact airfoil of finite thickness and arbitrary trailing edge geometry. For the flat plate, the radiation can be approximated by considering the diffraction at the edge of the boundary layer blocked pressure, which is assumed to convect in a frozen pattern past the edge. The same approximation for a thick airfoil significantly underpredicts the high-frequency components of the sound. In this case, the problem must be formulated in terms of the diffraction of the boundary layer "upwash" velocity. Both approaches are equivalent for the flat-plate airfoil, but the extension permits account to be taken of modifications of the turbulence during convection past the variable geometry edge.

In applications it is desirable to be able to make accurate predictions of low Mach number edge noise by first performing numerical simulations of the edge flow based on the equations for an *incompressible* fluid, and then inserting the results into a suitable surface integral representation of the radiated sound. When the airfoil chord is not acoustically compact, it is *not* possible to make such predictions solely from a knowledge of the incompressible approximation to the unsteady surface pressure. This is because the airfoil itself extends into the acoustic far field, and the prescribed surface pressure must contain sufficient *acoustic* information to ensure that the calculated radiation satisfies the appropriate dynamical boundary conditions on the airfoil. In order to satisfy these conditions using incompressible data, the surface integral should involve an acoustic Green's function that is specifically tailored to the boundary conditions. For a rigid airfoil the normal derivative of the Green's function should vanish on its surface, and the incompressible data required to determine the far-field sound is the boundary layer "upwash" velocity. This velocity is equal to that given by the (free-field) Biot–Savart formula applied to the boundary layer vorticity lying *outside* the viscous sublayer.

ACKNOWLEDGMENT

The work reported here is supported by the Office of Naval Research under Grant N00014-98-1-0798 administered by Dr. L. Patrick Purtell. The author gratefully acknowledges the benefit of discussions with Dr. William K. Blake during the preparation of this paper.

REFERENCES

1. W. K. Blake and J. L. Gershfeld 1989 *Lecture Notes in Engineering*, *Vol.* 46 (M. Gad-el-Hak, editor). *Frontiers in Experimental Fluid Mechanics*. The aeroacoustics of trailing edges.
2. T. F. Brooks, D. S. Pope and M. A. Marcolini 1989 *National Aeronautics and Space Administration Reference Publication No. 1218*. Airfoil self-noise and prediction.
3. D. G. Crighton 1991 *Aeroacoustics of Flight Vehicles*: *Theory and Practice*, (Vol. 1. *National Aeronautics and Space Administration Reference Publication No. 1258.* Airframe noise., Chapter 7.
4. M. S. Howe 1976 *Journal of Fluid Mechanics* **76**, 711–740. The influence of vortex shedding on the generation of sound by convected turbulence.
5. M. S. Howe 1986 *Proceedings of the Royal Society* **A 420**, 157–182. Contributions to the theory of sound production by vortex-airfoil interaction, with application to vortices with finite axial velocity defect.
6. N. Curle 1955 *Proceedings of the Royal Society* **A 231**, 505–514. The influence of solid boundaries upon aerodynamic sound.
7. J. E. Ffowcs Williams and D. L. Hawkings 1969 *Philosophical Transactions of the Royal Society* **A 264**, 321–342. Sound generation by turbulence and surfaces in arbitrary motion.
8. M. J. Lighthill 1952 *Proceedings of the Royal Society* **A 211**, 564–587. On sound generated aerodynamically. Part I: general theory.
9. M. J. Lighthill 1954 *Proceedings of the Royal Society* **A 222**, 1–32. On sound generated aerodynamically. Part II: turbulence as a source of sound.
10. J. E. Ffowcs Williams and L. H. Hall 1970 *Journal of Fluid Mechanics* **40**, 657–670. Aerodynamic sound generation by turbulent flow in the vicinity of a scattering half-plane.
11. D. M. Chase 1972 *Journal of the Acoustical Society of America* **52**, 1011–1023. Sound radiated by turbulent flow off a rigid hal-plane as obtained from a wavevector spectrum of hydrodynamic pressure.
12. K. L. Chandiramani 1974 *Journal of the Acoustical Society of America* **55**, 19–29. Diffraction of evanescent waves, with applications to aerodynamically scattered sound and radiation from unbaffled plates.
13. D. M. Chase 1975 *American Institute of Aeronautics and Astronautics Journal* **13**, 1041–1047. Noise radiated from an edge in turbulent flow.
14. R. K. Amiet 1976 *Journal of Sound and Vibration* **47**, 387–393. Noise due to turbulent flow past a trailing edge.
15. W. K. Blake 1986 *Mechanics of Flow–induced Sound and Vibration*, *Vol. 2*: *Complex Flow–Structure Interactions*. New York: Academic Press.
16. M. S. Howe 1978 *Journal of Sound and Vibration* **61**, 437–466. A review of the theory of trailing edge noise.
17. M. S. Howe 1998 *Department of Aerospace and Mechanical Engineering*, *Boston University*, *Report AM-98-001*. Reference manual on the theory of lifting surface noise at low Mach numbers.
18. J. C. Hardin and J. E. Martin 1997 *American Institute of Aeronautics and Astronautics Journal* **35**, 810–815. Flap side-edge noise: acoustic analysis of Sen's model.

19. B. Noble 1958 *Methods based on the Wiener–Hopf Technique for the Solution of Partial Differential Equations*. Oxford: Pergamon Press. (Reprinted 1988, Chelsea Publishing Company, New York).
20. M. Abramowitz and I. A. Stegun (editors) 1970 *Handbook of Mathematical Functions* (ninth corrected printing), *Applied Mathematics Series No. 55*. U.S. Department of Commerce, National Bureau of Standards.
21. M. S. Howe 1998 *Acoustics of Fluid–Structure Interactions*. Cambridge: Cambridge University Press.
22. D. M. Chase 1980 *Journal of Sound and Vibration* **70**, 29–67. Modeling the wavevector-frequency spectrum of turbulent boundary layer wall pressure.
23. G. M. Corcos 1964 *Journal of Fluid Mechanics* **18**, 353–378. The structure of the turbulent pressure field in boundary layer flows.
24. P. M. Morse and H. Feshbach 1953 *Methods of Theoretical Physics*, Vols. 1 and 2. New York: McGraw-Hill.
25. M. S. Howe 1975 *Journal of Fluid Mechanics* **71**, 625–673. Contributions to the theory of aerodynamic sound, with application to excess jet noise and the theory of the flute.
26. M. J. Lighthill 1958 *An Introduction to Fourier Analysis and Generalized Functions*. Cambridge: Cambridge University Press.
27. H. Lamb 1932 *Hydrodynamics* Cambridge: Cambridge University Press, sixth edition, (reprinted 1993).
28. W. K. Blake 1983 *Proceedings of the International Symposium on Turbulence Induced Vibrations and Noise of Structures* (M. M. Sevik, editor), 45–65. New York: American Society of Mechanical Engineers. Excitation of plates and hydrofoils by trailing edge flows.
29. J. Gershfeld, W. K. Blake and C. K. Knisely 1988 *American Institute of Aeronautics and Astronautics Paper* 88-3826-CP Trailing edge flow and aerodynamic sound.
30. J. O. Hinze 1975 *Turbulence*. New York: McGraw-Hill, second edition.
31. G. K. Batchelor and I. Proudman 1954 *Quarterly Journal of Mechanics and Applied Mathematics* **7**, 83–103. The effect of rapid distortion of a fluid in turbulent motion.
32. H. S. Ribner and M. Tucker 1953 *National Advisory Committee on Aeronautics* Report *No*. 1113. Spectrum of turbulence in a contracting stream.
33. H. Ashley and M. Landahl 1965 *Aerodynamics of Wings and Bodies*. Reading, MA: Addison-Wesley.
34. Y. C. Fung 1993 *An Introduction to the Theory of Aeroelasticity*. New York: Dover Publications Inc.